Design of filters in a one-dimensional tight-binding system

Bruno Lindquist
Department of Physics and Measurement Technology, Linköping University, SE-581 83 Linköping, Sweden
(Received 18 October 2000; published 12 April 2001)

We show how to design one-dimensional systems that in the transmission through a finite potential barrier, in a predetermined way, discriminate between monochromatic waves depending on their wave number. These systems, described by the on-site tight-binding equation, act as filters of different types, with adjustable pass and stop bands. The use of these filters for discrimination of linear wave packets depending on their different velocities is illustrated, and we also comment on the influence of an added nonlinearity.

DOI: 10.1103/PhysRevE.63.056605 PACS number(s): 71.15.Ap, 71.90.+q, 73.40.−c

I. INTRODUCTION

We consider here the on-site tight-binding equation with constant nearest-neighbor hopping

$$-\psi_{n+1}-\psi_{n-1}+V_n\psi_n=E\psi_n, \tag{1}$$

where n is the site index, V_n is the on-site potential, and the hopping integral is normalized to -1. This equation is equivalent to a discretized time-independent Schrödinger equation. This ubiquitous model and the connection between the nature of the eigenstates, the spectrum of allowed energies, the physical properties, and the choice of V_n as random [1] or deterministic aperiodic [2] have been most thoroughly studied. In this paper we will study the possibility of constructing a system obeying Eq. (1) that act as a discriminator of Bloch waves specified by certain wave numbers k. First the construction of a band-reject (BR) filter with low transmission in an interval $k_1 \leqslant k \leqslant k_2$ (the stopband) and high transmission outside this interval (the passbands) will be demonstrated. Also the transmission curve of a filter with the inverse characteristic, a band-pass (BP) filter, as well as filters with low-pass (LP) and high-pass (HP) characteristics will be shown. The discrimination of wave packets depending on their different velocities is illustrated.

The idea of constructing a filter of a certain type is based on the reflection of an initial plan wave $\propto e^{i(2\pi kn-E_k t)}$ by the Fourier components $\tilde{V}(k_p)$ of the lattice on-site potential. (The definition of the discrete Fourier transform DFT, could be found in the Appendix A.) Here E_k is the energy of the wave, while k_p denotes the lattice wave number. The contribution of k_p to the real potential V_n is (neglecting the normalization) the sum of $\tilde{V}(k_p)$ and $\tilde{V}(-k_p)$ [an asterisk denotes the complex conjugate, it naturally holds that $\tilde{V}(-k_p)=\tilde{V}^*(k_p)$]. Pure Bragg reflection ($k \leftrightarrow -k$) occurs when $|k_p|=2|k|$. At this condition the current [$J=2\,\mathrm{Im}(\psi_n\psi^*_{n-1})$] is periodically changing sign with the period $\propto 1/|\tilde{V}(k_p)|$. With increasing difference between k and the resonance criterion more and more k values are involved in the scattering process, even if there is only one initial plane wave and only one k_p value in the Fourier expansion of the potential (a cosine-formed potential). With more k_p values the problem is in general analytically not solvable even if the potential is periodic. Still worse if one has to take into account the spectral density of a wave packet. But the scattering at $|k_p| \cong 2|k|$ is by far of most importance, if the extension of the lattice is infinite and there are not too large values of the on-site potential. We have used this criterion in the construction of different filters adding Fourier components $\tilde{V}(k_p)$ to the lattice on-site potential with amplitudes and phases to give the best total effect on the transmission curve. If we, however, deal with the transmission through a barrier the borders play an essential role. Too step borders at the entrance and the exit sides of the barrier lead to large reflections at the borders, resulting in interference, giving peaks and valleys (ripple) in the transmission curve. With a barrier size of N sites, this ripple has the period $\Delta k \approx 1/2N$ (cf. the Ramsauer effect) and is not desirable, as we want as flat characteristic as possible in the stop and pass bands. So the wish is to have smooth borders if possible. In Sec. II the transmission of a plane wave is first derived and then successive improvements in the construction of the barrier are investigated. The effects on wave packets are dealt with in Sec. III, where the influence of an added nonlinearity is also considered. We will in the following use the terminology that the ''left'' is toward the low n side.

II. STATIONARY TRANSMISSION

The system that will be considered here is described by Eq. (1), and consists of a finite aperiodic chain (a potential barrier when $1 \leqslant n \leqslant N$), embedded in an infinite periodic chain with $V_n \equiv 0$. We will first study the problem of stationary transmission through this barrier, when the wave functions outside the barrier are taken as single Bloch waves specified by a wave number k. By stationary transmission we here simply mean that the probability $|\psi_n|^2$ and the probability current are time independent in contrast to the case when the transmission of a wave packets is studied. With R_0, R_1, and T_0 defining the incoming, reflected, and outgoing wave amplitudes, respectively, we have the following relations:

$$\begin{aligned}
&\psi_n = R_0 e^{i2\pi kn} + R_1 e^{-i2\pi kn}, \quad n \leqslant 1,\\
&-\psi_{n+1}-\psi_{n-1}+V_n\psi_n = E\psi_n, \quad 1 \leqslant n \leqslant N,\\
&\psi_n = T_0 e^{i2\pi kn} + T_1 e^{-i2\pi kn}, \quad N \leqslant n,
\end{aligned} \tag{2}$$

where $T_1 \equiv 0$ in the present context.

The relation $E=-2\cos(2\pi k)$ is valid for a Bloch wave outside the barrier and is used also inside the barrier, which is motivated by the infinite chain and that Eq. (1) is valid for all n. In the usual way the transmission coefficient t is defined as

$$t=\frac{|T_0|^2}{|R_0|^2}. \tag{3}$$

The complex wave function ψ gives by Eq. (1) rise to a real four-dimensional mapping. This mapping can be reduced to a two-dimensional one [3,2] by the use of current conservation $[J=2\ \mathrm{Im}(\psi_n\psi_{n-1}^*)=2|T_0|^2\sin(2\pi k)]$. By defining the two quantities

$$x_n=\frac{|\psi_n|^2}{|T_0|^2},\quad y_n=\frac{\mathrm{Re}(\psi_n\psi_{n-1}^*)}{|T_0|^2}, \tag{4}$$

the reduced mapping will take the form

$$x_{n-1}=\frac{1}{x_n}[y_n^2+\sin^2(2\pi k)],\quad \forall n,$$

$$y_{n-1}=-y_n+x_{n-1}(V_{n-1}-E),\quad 2\leqslant n\leqslant N+1, \tag{5}$$

where the initial conditions are $x_{N+1}=1$, $y_{N+1}=\cos(2\pi k)$. By iterating Eq. (5) from the output end to the input end of the barrier and using Eqs. (2) and (4) the transmission coefficient is by Eq. (3) obtained as

$$t=\frac{4\sin^2(2\pi k)}{x_1+x_0-2y_1\cos(2\pi k)+2\sin^2(2\pi k)}. \tag{6}$$

First three comments on the general characteristics of $t(k)$: (1) An inspection of Eq. (6) reveals that $t(k)$ is unaffected by the simultaneous substitution $k\to 0.5-k$, $V_n\to -V_n$. That is, $V_n\to -V_n$ mirror $t(k)$ in $k=0.25$. (2) The transmission curve is the same independent of which side of the barrier the wave is coming from. This is due to the invariance of the Schrödinger equation under time reversal. (See Appendix B for a derivation of this characteristic.) (3) From the preceding two characteristics it follows that $t(k)$ is symmetric around $k=0.25$, if the potential is antisymmetric under inversion with respect to the middle of the barrier ($V_n=-V_{N+1-n}$). If N is odd, the middle lattice site must have zero on-site potential. In the following, we use this definition of an ''antisymmetric'' potential.

If we want to design the real V_n of the barrier in the way that *all* components of its discrete Fourier transform have the same amplitude (except for the constant one), this is done as

$$V_n=\sum_{p=1}^{[N/2]}A_p\sin\left(\frac{2\pi pn}{N}+\phi_p\right),\quad k_p=p/N. \tag{7}$$

where the upper limit $p=N/2$ (for N even) or $(N-1)/2$ (for N odd). Except for the highest component $p=N/2$ (for N even) the independent random phases ϕ_p are uniformly distributed in the interval $[0,\ 2\pi]$ and the amplitudes are constant, i.e., $A_p=A$. When $p=N/2$, which corresponds to only one component in the DFT (whereas the other p values correspond to two components), we, however, take $\phi_{N/2}=\pm\pi/2$ and $A_{N/2}=A/2$ to get the same amplitude in the DFT. Note that the constant contribution from $p=0$ is excluded from Eq. (7), giving $\langle V_n\rangle=0$. In what follows the potential is normalized to have the root mean square (rms) value $V=\sqrt{\langle V_n^2\rangle}$. This normalization means that, if V constant, the amplitude of any component in Eq. (7) changes approximately as $A\propto 1/\sqrt{N}$. The Fourier transform method to obtain the potential has recently [4] been used to give a power law relation $A_p^2\propto 1/k_p^\alpha$. It was found that for $\alpha<2$ all one-electron states are localized, but there is a finite range of energy values with extended eigenstates for $\alpha>2$.

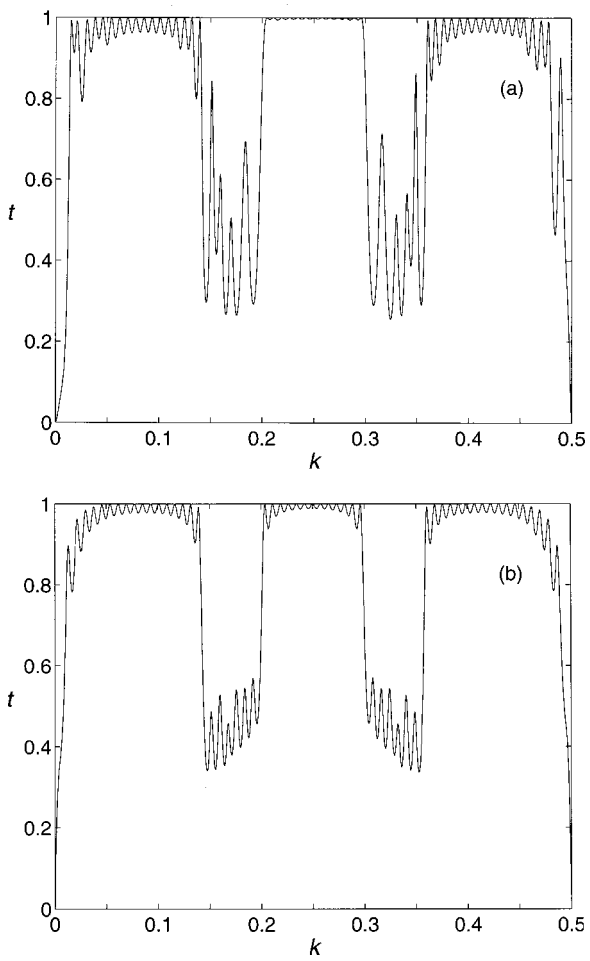

FIG. 1. The transmission coefficient t as a function of k with the on-site potential chosen according to Eq. (7) but with only $0.3\leqslant k_p\leqslant 0.4$ included in the summation, i.e., a first approximation of a BR-filter with stopband $0.15\leqslant k\leqslant 0.2$. The RMS value $V=0.1$ and $N=64$. (a) One single realization with random phases ϕ_p. (b) The result after averaging over 100 realizations with random ϕ_p.

In Fig. 1 the first illustrative design of a band-reject filter with stop band $0.15\leqslant k\leqslant 0.2$ is shown. From Eq. (7) only the values $k_p=2k$ for k values in the stop band are included in the summation. With changed values of the parameters N and V the complimentary bandpass filter with passband $0.15\leqslant k\leqslant 0.2$ is shown in Fig. 2. Here the corresponding values of k_p are excluded from the summation. Figures 1(a)

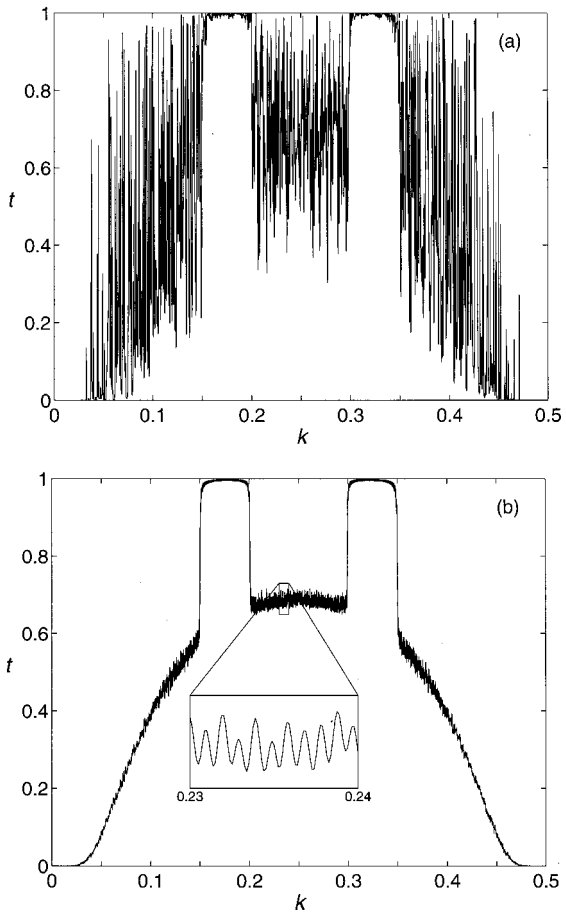

FIG. 2. The transmission coefficient t as a function of k with the potential chosen according to Eq. (7) but with $0.3 \leqslant k_p \leqslant 0.4$ excluded from the summation, i.e., a first try to design a BP-filter with passband $0.15 \leqslant k \leqslant 0.2$. The RMS value $V=0.05$ and $N=512$. (a) One single realization with random ϕ_p. The potential could be seen at the top of Fig. 6. (b) The result after averaging over 1000 realizations with random ϕ_p. Inserted: An enlargement of a small interval showing the ripple caused by the borders.

and 2(a) show the large fluctuation in the transmission curve in single realizations; even with some peaks with nearly perfect transmission in the supposed stop band in Fig. 2(a). That is, the random phases ϕ_p are not good choices although the averaging over several realizations in Figs. 1(b) and 2(b) show some desired BR and BP characteristics, respectively. But, of course, filters cannot rely on averaging; they have to work in every single realization. The averaged characteristics exhibit some interesting features: *First, the ripple* caused by the borders is clearly seen in Fig. 1(b), while the ripple in Fig. 2(b) has a smaller amplitude and the average needs to be taken over more realizations to become clearly visible. With shorter length of the barrier (here $N=64$ and $N=512$, respectively) the influence of the borders generally increases at the expense of the bulk. *Second*, the *overall* transmission in the different bands is not at all as flat as desired, i.e., the influence on $t(k)$ depends on k_p even if all amplitudes A_p are equal. In large intervals of t and k the relation $t(k_p/2) \propto 1/\sin(\pi k_p)$ is valid. This is reflected in the stopband of the BP filter and in the passband of the BR filter (although this

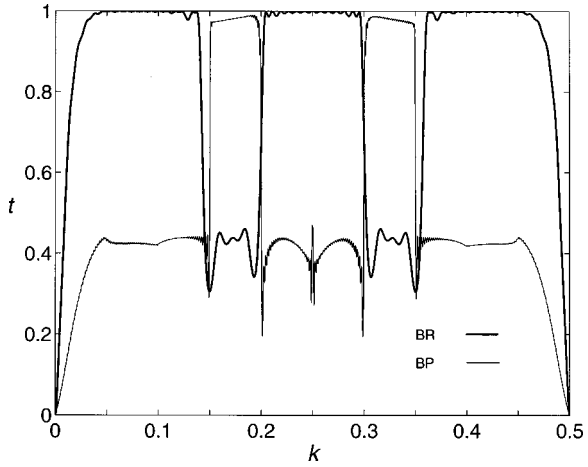

FIG. 3. The transmission curve of a BR-filter (BP-filer) with stopband (passband) $0.15 \leqslant k \leqslant 0.2$. The potential is generated according to Eq. (8) and the different phases chosen as $\phi_p = p\pi$. Compare with Fig. 1 (2) where the parameters $V=0.1$ (0.05) and $N=64$ (512) are the same as here.

feature actually is better studied in potentials with more separated peaks in the Fourier transform of the potential, or even with one single Fourier component at a time). The relation holds if t not too close to $t=0$ or $t=1$, nor must the wave number be close to $k=0$ (or $k=0.5$). These conditions on k mean that the current $J \propto \sin(2\pi k)$, or if a wave packet the kinetic energy [5] of the packet, must be large compared to the on-site potential. If not so the case, the wave (or wave packet) is scattered more independently by the different (*local*) V_n and has no possibility to ''sense'' the *global* characteristics expressed by the different $\tilde{V}(k_p)$.

A better design of the potential in the barrier is thus

$$V_n = \sum_{p=1}^{[N/2]} A_p \sin\left(\frac{2\pi p n}{N} + \phi_p\right) \sin\left(\frac{\pi p}{N}\right), \quad k_p = p/N, \quad (8)$$

with the different deterministic phases chosen as $\phi_p = p\pi$. This choice of phases makes the potential more focused to the middle of the barrier (i.e., on the average larger values of $|V_n|$ in this region) and makes the borders become more smooth and hence cause a reduction of the ripple. As a side effect the potential in the barrier becomes almost antisymmetric, with the result that the transmission $t(k)$ becomes even more symmetric around $k=0.25$ than with independent random phases ϕ_p. A linear dependent $\phi_p = pC_1$, with $C_1 \neq \pi$, just change the point of focusing n_f, and does not change the transmission curve drastically as long as n_f is not near the borders. Figure 3 demonstrates the effect on the transmission curves of the BR and BP filters shown in Figs. 1 and 2 when the potential is given by Eq. (8) and the different phases by $\phi_p = p\pi$. In these single realizations, the most remarkable improvement in the characteristics are perhaps that the ripple caused by the borders is greatly removed from the shorter BR filter and in the flattening of the BP filter characteristic.

When we want to proceed to improve the filter characteristics, we have to compromise between different qualities

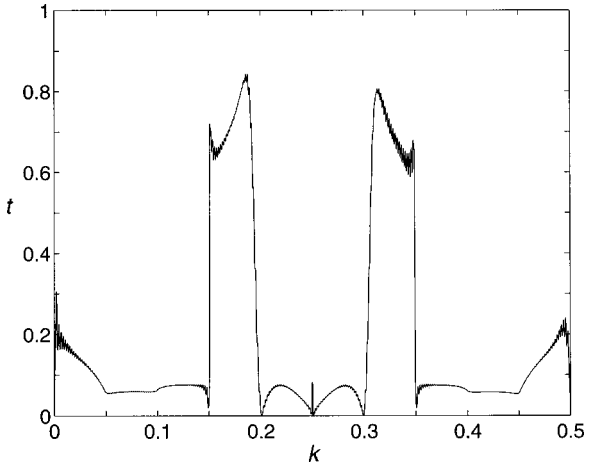

FIG. 4. The influence on the transmission curve of the BP-filter shown in Fig. 3 when the potential strength is increased from $V=0.05$ to $V=0.1$, while everything else is unchanged. The potential is shown in the middle of Fig. 6.

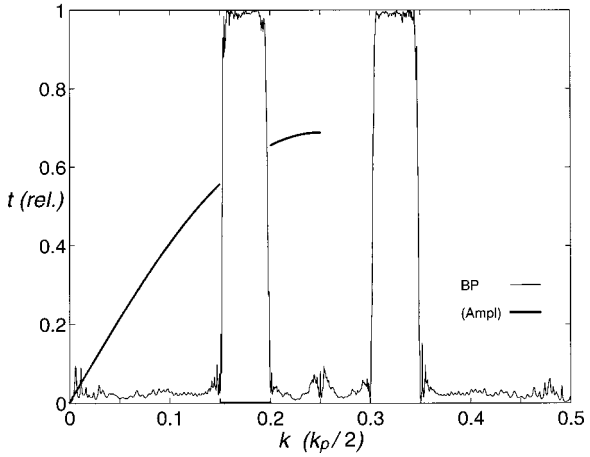

FIG. 5. The transmission curve of a BP-filter with passband $0.15 \leqslant k \leqslant 0.2$ when the potential is generated according to Eqs. (8) and (9). The nonlinearity parameter in the determination of ϕ_p is $C_2=0.8°$, while $V=0.1$ and $N=512$. Also shown are the Fourier amplitudes $|\tilde{V}(k_p)|$ of the potential in a relative scale. Note that the scale of k_p is compressed relative that of k. This brings out the scattering of the waves that occur when $|k_p|=2|k|$. Compare the transmission with the BP-filter in Figs. 3 and 4 where the potentials have the same relative amplitude characteristics as here. The potential is shown at the bottom of Fig. 6.

such as high (low) transition in the pass bands (stop bands), maximally flat pass bands, and steep sloops in $t(k)$ in the transition between pass bands and stop bands. To decrease the transmission in the stop bands, for a fixed length of the barrier, we want to increase the strength V of the potential. This must be done, in a way that the focusing of the potential to the middle of the barrier is reduced. Otherwise the larger values of $|V_n|$ in this region with increasing V, lead to increasing interference between the *local* potential barriers. This, e.g., tends to deteriorate the transmission in the pass bands. (In Fig. 4 the effect of doubling of V is shown for the BP filter in Fig. 3.) A way to control the amount of focusing of the potential is to introduce a nonlinear term in the choice of the different phases. By numerical investigation of different forms of $\phi_p(p)$ we have found a simple quadratic form best suited in most cases:

$$\phi_p = p\pi + C_2(p - p_{m,i})^2, \tag{9}$$

where C_2 is a constant, and with p belonging to stop band No. i, then $p_{m,i}$ is the number of the middle term belonging to this stop band. The parameter C_2 has to been chosen in each separate case (type of filter, potential strength, etc.) to give the (subjectively) best total characteristic. The greatly improved effect on the transmission of including the nonlinear term in ϕ_p is shown in Fig. 5, with our previously used BP filter as an example. For the BP filter the focusing of the potential to the middle of the barrier when $\phi_p = p\pi$ and the defocusing when C_2 is included is shown in Fig. 6, where also an example of the potential when ϕ_p is randomly chosen is seen. Two more examples of filters where the potentials are determined by Eqs. (8) and (9) are shown in Fig. 7. Filters with a pass band at low k ($k<0.05$) are the most difficult type to obtain, as $k \to 0$ always means that $t \to 0$.

The BR filter with the narrowest stop band is obtained if only one periodic term is used to generate the potential. This is a so-called ''notch filter'' of which an example could be seen in Fig. 8. The notch becomes narrower if the width N of the array is increased and to have as narrow notch as possible the strength V of the potential should not be increased over the point where the minimum in transition is near zero. The ripple in the transition seen in Fig. 8 is caused by the potential at the borders. The ripple at the end points ($k<0.05$ and $k>0.45$) could almost completely be removed if the phase ϕ_p is changed from zero to some value ($\phi_p = \pi/2 - \pi k_p$,

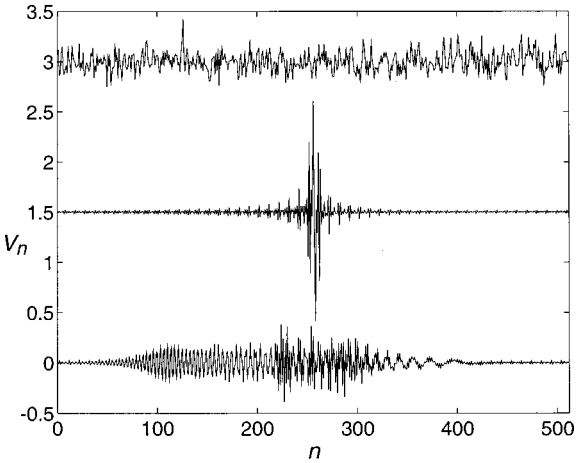

FIG. 6. The on-site potential, V_n, of the BP-filters, with passband $0.15 \leqslant k \leqslant 0.2$ and $N=512$ used as examples in the previous Figs. The potentials are from top to bottom in the figure related to the parameters used in Figs. 2a, 4, and 5, respectively. To simplify comparison the upper random potential is rescaled so that $V=0.1$ in all three cases. The upper two curves are drawn with offsets in V_n of 1.5 and 3 respectively. Notice the quite different spatial appearance of the potentials. All three are resulting in the same type of filter, the potential at the bottom with the best characteristics.

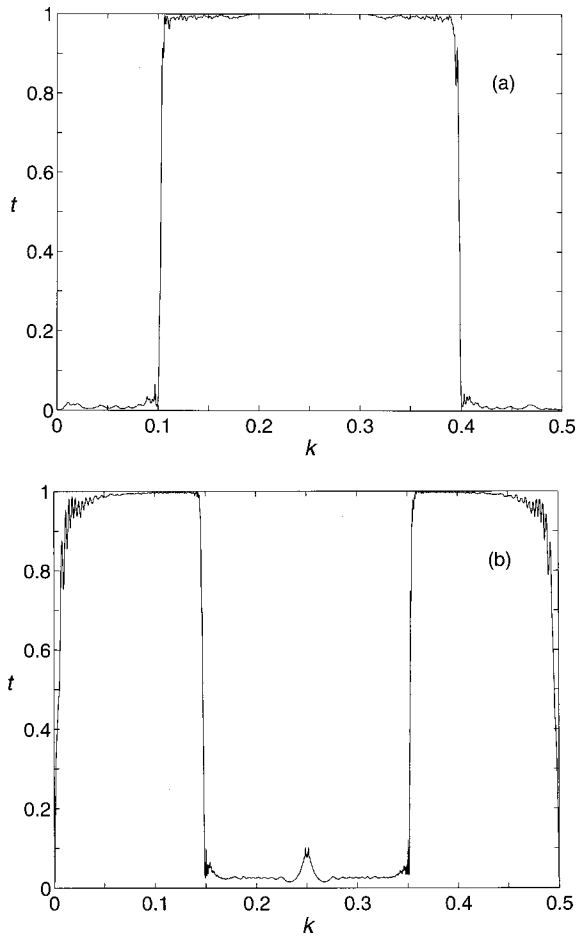

FIG. 7. The transmission coefficient t as a function of k of two different types of filters when the potentials are generated according to Eqs. (8) and (9). (a) HP-filter with passband $k \geqslant 0.1$, $V=0.06$, $C_2=1.9°$, and $N=256$; (b) LP-filter with passband $k \leqslant 0.15$, $V=0.1$, $C_2=0.94°$, and $N=512$.

modulo π). (This gives a symmetric potential under inversion with respect to the middle of the barrier.) *All* of the ripple, however, could be removed by the application of some tapering factor on the potential. A technique sometimes used in spectral analysis to remove or reduce the terminal discontinuities of sampled data. In example the multiplication of V_n by a Hamming window [6] [i.e., the weighting factor $w(n)=0.54-0.46\cos(2\pi n/N)$] will remove the entire ripple in Fig. 8 on the expense of some broadening of the notch. The applying of a tapering factor, however, means the introduction of new components in the Fourier spectrum of the potential. In the other types of filters studied here, the window technique is found not to be applicable, because of the deformation of the initial Fourier spectrum with ''unpredictable'' influence on the transition curve as a result.

III. TRANSMISSION OF WAVE PACKETS

Up to now we have dealt with the transmission coefficient t of a plane wave as a function of the wave number k. In a *linear* system, the transmission of a wave packet ψ_n with spectral density $P(k)$ (its DFT) is obtained by averaging

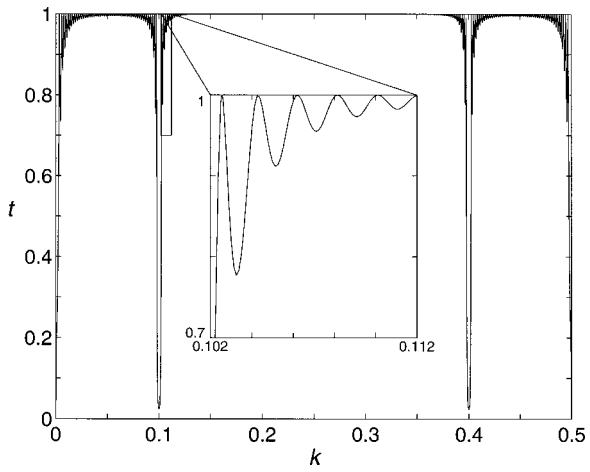

FIG. 8. An example of the transmission curve of a BR-filter with the narrowest ''stopband'' for a certain length N of an array. Here only one component with $k_p=0.2$ is used when generating the potential and the parameters are $\phi_p=0$, $V=0.017$, and $N=250$. Inserted is an enlargement of a small interval showing the ripple, with a period $\Delta k \approx 1/2N=0.002$, caused by the borders. The figure is further discussed in the text.

over all k in the, toward the barrier, incoming packet,

$$\langle t \rangle = \int |P(k)|^2 t(k) dk \Big/ \int |P(k)|^2 dk. \qquad (10)$$

If the wave packet has the carrier wave number $k_c=k$, i.e., $\psi_n=|\psi_n|e^{i2\pi kn}$, the spectral density is concentrated around k and we define the transmission coefficient of the wave packet as $t(k_c)=t(k)=\langle t \rangle$. With spatially extended and reasonable shaped wave packets, $t(k)$ is qualitatively the same as that of a plane wave as $P(k)$ in these cases is strongly localized around k_c. With a Gaussian-shaped $|\psi_n|^2$ with a width given by its standard deviation σ, the also Gaussian-shaped $|P(k)|^2$ has a standard deviation $\sigma_k \approx 1/(4\pi\sigma)$. (This relation is exact in the continuous limit.) The effect of the averaging is exemplified in Fig. 9 where, calculated by Eq. (10), the transmission of an incoming Gaussian-shaped wave with $\sigma=16$ is shown. We have in this article preferred to study rather short lengths of the barriers for two reasons. First, it is a greater challenge to design filters with good total characteristics with short barriers. Second, when dealing with wave packets the length of the barrier could be chosen, depending on the width of the packets, so that the ripple is smoothed.

It could be off interest to investigate the effect on the transmission of wave packets through the barrier, of an added (cubic) nonlinearity in the used model equation. In the nonlinear case, where the previous method cannot be used, we change to numerical calculations by solving the time-dependent discrete nonlinear Schrödinger equation

$$i\frac{\partial}{\partial t}\psi_n = -\psi_{n+1}-\psi_{n-1}+V_n\psi_n+\alpha|\psi_n|^2\psi_n, \qquad (11)$$

where α is the nonlinearity parameter. The nonlinearity is assumed to exist only in the barrier (i.e., when $1 \leqslant n \leqslant N$) and the wave packet is launched immediately outside the

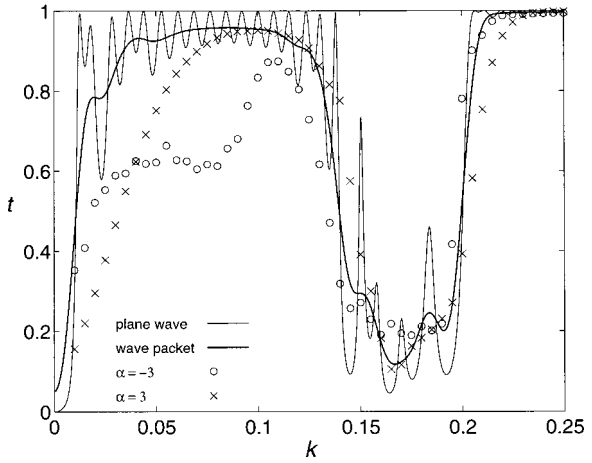

FIG. 9. The effect of the averaging of $t(k)$ (valid for a plane wave) when the incoming wave packet is Gaussian shaped with standard deviation $\sigma=16$, corresponding to a Gaussian shaped averaging factor $|P(k)|^2$ with standard deviation $\sigma_k \approx 1/(4\pi\sigma) \approx 0.005$. The on-site potential is chosen as in Fig. 1(a), i.e., the first approximation of a ''BR-filter'' with stopband $0.15 \leqslant k \leqslant 0.2$, $V=0.1$, $N=64$, and random phases ϕ_p. Only the interval $0 \leqslant k \leqslant 0.25$ is shown, as $t(k)$ in Fig. 1(a) is almost symmetric around $k=0.25$. The wave packet is spatial narrow enough to cancel the ripple caused by the borders. With this wave packet also two cases of the effect (further discussed in the text) of an added nonlinearity are shown. The nonlinearity parameter $\alpha=\pm 3$ respectively.

barrier on the left side. To integrate Eq. (11) we use a method previously found to be very reliable [5,7] and here the difference, when $\alpha=0$, between the result of Eq. (10) and by integrating Eq. (11) is negligible (i.e., it would not be visible in Fig. 9). An example of the effect of the added nonlinearity is shown in Fig. 9 for both a negative and a positive value of the nonlinearity parameter. Only the interval $0 \leqslant k \leqslant 0.25$ is shown. In the linear case $t(k)$ is almost symmetric around $k=0.25$, and there would have been perfect symmetry if the potential had been antisymmetric. When $\alpha \neq 0$ the symmetry is broken, even with an antisymmetric potential. With every potential, however, $t[k,\alpha,V(n)]$ is a mirror in $k=0.25$ of $t[k,-\alpha,-V(n)]$. The reason is that the time evolution of $|\psi_n|^2$ is unchanged if we make the simultaneous transformation

$$k \rightarrow 0.5-k, \quad V_n \rightarrow -V_n, \quad \alpha \rightarrow -\alpha, \tag{12}$$

which, by putting $\psi_n = c_n e^{i2\pi kn}$, could be seen from Eq. (11) and its complex conjugate counterpart. There has been much activity to form an understanding of nonlinear systems. See, for instance, Ref. [8] (for an introductory review) and Ref. [9]. An exhaustive description of the influence of the nonlinearity on the transmission of the different ''filters'' studied here is difficult to give. The task is worth a further study, but is beyond the scope of this article. After investigated many types of potential barriers, looking for which combinations of parameters are leading to increasing/decreasing transmission, we have, however, found one common characteristic. In regions of k where $(\partial/\partial k)t(k)|_{\alpha=0} > 0$ (i.e., going from a stop band to a pass band with increasing k), $t(k)$ is decreased (increased) if $\alpha > 0 (\alpha < 0)$. On the contrary, in regions where $(\partial/\partial k)t(k)|_{\alpha=0} < 0$, $t(k)$ is increased (decreased) if $\alpha > 0 (\alpha < 0)$. The effect on the transmission curve is that it seems to move towards higher (lower) k values when α is increased (decreased). This effect, which is exemplified in Fig. 9, appears for all k in the interval $0 < k < 0.5$ except ''near'' $k=0$ or $k=0.5$ (i.e., slowly moving wave packets with low kinetic energy). At present we have no valid argument for the reason of these shifts in the transmission curves. We have, however, in some cases examined the local Fourier transform, of the wave packet *in* the barrier, during the scattering process. The observed scattering of the initial Fourier components is with $\alpha > 0$ ($\alpha < 0$) more pronounced toward lower (higher) k values. This could give the observed shift in the transmission curve. But, if this asymmetry of the scattering is a general fact, is presently unclear. If so, there is still the open question of the reason for the asymmetry.

IV. CONCLUDING REMARKS

We have shown how to design filters that discriminate between wave packets depending on their velocities. With the given examples as guidelines it is possible to design filters for plane waves with almost any location of the pass band(s) in the transmission coefficient. The effect of the designed filter on a wave packet with known spatial form could then quite easily be estimated. However, filters with a pass band down to ''very low'' velocities are the most difficult to design as there is always a cut of velocity for energetical reasons. This type of filter requires low on-site potentials and therefore a long barrier to get the desired low transition in the stop band. The resulting characteristic of all filters is always a compromise between different wanted features.

The effect of an added nonlinearity is that the characteristics are less predictable, and often the good qualities of the transmission curve are deteriorated. The transmission curve appears to be shifted in the k direction with changed nonlinearity.

ACKNOWLEDGMENT

The author would like to thank Rolf Riklund for clarifying discussions about physics in general. Financial support from the Swedish Natural Science Research Council is also gratefully acknowledged.

APPENDIX A: THE DISCRETE FOURIER TRANSFORM

The discrete Fourier transform (DFT) and the corresponding inverse transform is here defined as

$$X(k) = \frac{1}{N}\sum_{n=1}^{N} x(n) e^{-i2\pi kn}, \quad 0 \leqslant k \leqslant 1-1/N, \quad \Delta k = 1/N.$$

$$x(n) = \sum_{\nu=0}^{N-1} X(k) e^{i2\pi kn}, \quad k=\nu/N, \quad 1 \leqslant n \leqslant N,$$

respectively. It is often preferable to think of the Fourier components in the interval $0.5<k\leqslant 1-1/N$ mapped on the negative interval $-0.5+1/N\leqslant k<0$.

APPENDIX B: SYMMETRY OF THE TRANSMISSION

We will, by the help of time reversal, show that the transmission coefficient is the same for waves coming from the left or right side toward the barrier, independent of the form of the potential. In Eq. (2) the plane waves to the left and right side of the barrier are joined by the linear conditions in the barrier. The joining conditions lead to two linear homogeneous relations between the coefficients R_0, R_1, T_0, and T_1. Hence a matrix M exists such that

$$\begin{pmatrix} R_0 \\ R_1 \end{pmatrix} = \begin{pmatrix} m_{11} & m_{12} \\ m_{21} & m_{22} \end{pmatrix} \begin{pmatrix} T_0 \\ T_1 \end{pmatrix}. \tag{B1}$$

With the wave incoming from the left, R_0, R_1, and T_0 are the incoming, reflected, and outgoing wave amplitudes, while $T_1=0$. In this case the transmission coefficient is

$$t_L = t = \frac{|T_0|^2}{|R_0|^2} = 1/|m_{11}|^2 \tag{B2}$$

and the reflection coefficient is $r_L=r=|R_1|^2/|R_0|^2 = |m_{21}|^2/|m_{11}|^2$.

Current conservation $t+r=1$ then gives

$$|m_{11}|^2 - |m_{21}|^2 = 1. \tag{B3}$$

The time-reversed solution corresponding to Eq. (2) is (with $\Phi_n=\psi_n^*$)

$$\Phi_n = R_0^* e^{-i2\pi kn} + R_1^* e^{i2\pi kn}, \quad n\leqslant 1,$$

$$-\Phi_{n+1} - \Phi_{n-1} + V_n\Phi_n = E\Phi_n, \quad 1\leqslant n\leqslant N.$$

$$\Phi_n = T_0^* e^{-i2\pi kn} + T_1^* e^{i2\pi kn}, \quad N\leqslant n.$$

Now if $R_1^* e^{i2\pi kn}$ is incident from the left, R_0^*, and T_1^* is defining the reflected and outgoing wave amplitudes, while $T_0^*=0$. Comparing with Eqs. (2) and (B1) we get

$$\begin{pmatrix} R_1^* \\ R_0^* \end{pmatrix} = \begin{pmatrix} m_{11} & m_{12} \\ m_{21} & m_{22} \end{pmatrix} \begin{pmatrix} T_1^* \\ T_0^* \end{pmatrix}$$

or, equivalently,

$$\begin{pmatrix} R_0 \\ R_1 \end{pmatrix} = \begin{pmatrix} m_{22}^* & m_{21}^* \\ m_{12}^* & m_{11}^* \end{pmatrix} \begin{pmatrix} T_0 \\ T_1 \end{pmatrix}.$$

This has the same form as Eq. (B1) and hence the two $\times 2$ matrices are equal, i.e., $m_{11}=m_{22}^*$ and $m_{12}=m_{21}^*$. This gives

$$M = \begin{pmatrix} m_{11} & m_{12} \\ m_{12}^* & m_{11}^* \end{pmatrix},$$

and with Eq. (B3) that $\det(\boldsymbol{M})=1$. The inverse can thus be written as

$$\boldsymbol{M}^{-1} = \begin{pmatrix} m_{11}^* & -m_{12} \\ -m_{12}^* & m_{11} \end{pmatrix}.$$

From Eq. (B1) we get

$$\begin{pmatrix} T_0 \\ T_1 \end{pmatrix} = \begin{pmatrix} m_{11}^* & -m_{12} \\ -m_{12}^* & m_{11} \end{pmatrix} \begin{pmatrix} R_0 \\ R_1 \end{pmatrix}.$$

Now let $T_1 e^{-i2\pi kn}$ be a wave incident from the *right*, T_0, and R_1 defining the reflected and outgoing wave amplitudes, while $R_0=0$. In this case the transmission coefficient is

$$t_R = \frac{|R_1|^2}{|T_1|^2} = 1/|m_{11}|^2,$$

which is equal to t_L, the transmission coefficient when the wave is incident from the *left* in Eq. (B2).

[1] *IOP Conference Proceedings No. 108, Localisation 1990*, edited by K. A. Benedict and J. T. Chalker (Institute of Physics, Bristol, 1991).

[2] M. Johansson and R. Riklund, Phys. Rev. B **49**, 6587 (1994), and references therein.

[3] Y. Wan and C. M. Soukoulis, Phys. Rev. B **40**, 12 264 (1989); Phys. Rev. A **41**, 800 (1990).

[4] F. A. B. F. de Moura and M. L. Lyra, Phys. Rev. Lett. **81**, 3735 (1998); Physica A **266**, 465 (1999); J. W. Kantelhardt *et al.*, Phys. Rev. Lett. **83**, 198 (1999); F. A. B. F. de Moura and M. L. Lyra, *ibid.* **83**, 199 (1999).

[5] B. Lindquist, M. Johansson, and R. Riklund, Phys. Rev. B **50**, 9860 (1994).

[6] F. J. Harris, Proc. IEEE **66**, 51 (1978).

[7] B. Lindquist and R. Riklund, Phys. Rev. B **56**, 13 902 (1997).

[8] *Introduction to Nonlinear Physics*, edited by L. Lam (Springer, Berlin, 1997).

[9] K. Ø. Rasmussen, D. Cai, A. R. Bishop, and N. Grønbech-Jensen, Europhys. Lett. **47**, 421 (1999), and references therein.